Stability-instability transition of reaction fronts in thermal oxidation of silicon

Hiroo Omi,[1,*] Hiroyuki Kageshima,[1] Tomoaki Kawamura,[1,†] Masashi Uematsu,[1,‡] Yoshihiro Kobayashi,[1,§] Seiji Fujikawa,[2,‖] Yoshiyuki Tsusaka,[2] Yasushi Kagoshima,[2] and Junji Matsui[3]
[1]*NTT Basic Research Laboratories, NTT Corporation, Atsugi 243-0198, Japan*
[2]*Graduate School of Material Science, University of Hyogo, 3-2-1 Kouto, Kamigori, Ako, Hyogo 678-1297, Japan*
[3]*Center for Advanced Science and Technologies, 3-1-1 Kouto, Kamigori, Ako, Hyogo 678-1205, Japan*
(Received 8 December 2008; revised manuscript received 15 May 2009; published 22 June 2009)

By combining atomic force microscopy and x-ray reflectivity measurements, the morphological evolution at the SiO_2/Si(001) interface during thermal silicon oxidation was systematically studied as a function of oxidation temperatures. We found that the oxidation-induced roughening switches to smoothening at an oxidation temperature of 1250 °C on the oxidation front. The transition is governed by how the strain induced by oxidation is spatially relieved at the interfaces in the silicon oxide bulk film through the interfacial transition layers, which is inevitably important for the strain-relief mechanism.

DOI: 10.1103/PhysRevB.79.245319 PACS number(s): 68.55.J−, 68.35.Ct, 68.35.Fx, 82.65.+r

I. INTRODUCTION

Thermal silicon oxidation is important not only for the formation of gate dielectric oxide films on a silicon surface but also for size control of silicon nanostructures.[1–4] Therefore, the modeling of oxidation kinetics has been extensively explored on planar silicon surfaces[2,3,5] and at the interface between growing silicon oxide film and planar[6–11] or nanoscale silicon surfaces.[4] Thanks to recent *in situ* experiments and theoretical calculations,[12,13] our understanding of the silicon oxidation kinetics at the interface between thermal silicon oxide and Si(001) has progressed considerably. For surface oxidation, the thermal oxidation can be categorized into two domains—active oxidation (etching) and passive oxidation (oxide growth)—depending on the oxygen pressure and the oxidation temperature.[14] However, the morphological stability of the growing interface, i.e., the reaction fronts in the growth regime, which governs roughening at the interface, has been not well clarified yet.

Concerning the growth front stability, it is well known that the change in the interface roughening and smoothening during the oxidation is mainly limited by interface reactions at oxidation temperatures of 800 °C and 1000 °C.[15,16] However, interface diffusion plays an important role at oxidation temperatures above 1200 °C.[17,18] Previously, quantitative modeling of the oxidation kinetics at the interface has been studied.[16,18] Chen and Gibson,[16] for instance, showed that the interface oxidation kinetics at an oxidation temperature of 900 °C should be written as the Langevin equation

$$\frac{\partial h(\mathbf{r},t)}{\partial t} = \mu \nabla^2 h(\mathbf{r},t) + \eta(\mathbf{r},t), \tag{1}$$

where t is the oxidation time, $h(\mathbf{r},t)$ is the interface height, μ is a constant, and $\eta(\mathbf{r},t)$ is a noise term describing the silicon oxidation, which is considered to happen randomly at silicon atom sites. The oxidation model indicates that oxygen atoms randomly form SiO_2 islands on the terrace shown in the second term on the right side, but that the resulting roughness is smoothened by the first term. Omi *et al.* recently performed scaling analyses of the roughening of the thermal oxidation at the oxidation temperature of 1200 °C and found that the lateral diffusion of silicon species at the interface, $\nabla^4 h$, should be added to Eq. (1) as follows:

$$\frac{\partial h(\mathbf{r},t)}{\partial t} = \mu \nabla^2 h(\mathbf{r},t) - D\nabla^4 h(\mathbf{r},t) + \eta(\mathbf{r},t), \tag{2}$$

where D is a constant.[18] They verified this by finding a phase transition in the universality class from the disordered to the step-terrace structure at the interface at oxidation temperatures between 1150 °C and 1380 °C.[18]

It is well known, on the other hand, that the thermal oxidation produces compressive stress in the oxide film and tensile stress in the silicon wafer due to the volume expansion and the difference in the thermal-expansion coefficients between Si and SiO_2.[2,3,19] The stress generated by the thermal oxidation is partially relieved by the formation of interfacial transition layers.[2,3,19] Therefore, the interface stress is an important candidate for the origin of interface roughening. Indeed, several researchers[19,20] have reported analyses of the stability of the planar interface during thermal silicon oxidation at low temperature (900 °C) with no viscous-flow effect and predicted that the elastic stress at the interface can make it dynamically unstable (roughening effect); diffusion and interfacial tension can make the planar interface stable during oxidation (smoothening effect). However, despite the theoretical prediction, the stress effect on the oxidation kinetics is not clearly evidenced in experiments and we are thus missing the stress effect on the oxidation kinetics in Eqs. (1) and (2).

In this work, to reveal whether the interface stress affects the stability of oxidation fronts or not, we systematically explore the details of the roughening at the interfaces in thermal silicon oxide films on Si(001) as a function of oxidation temperature by combining atomic force microscopy (AFM) (destructive method) and synchrotron x-ray reflectivity measurements (XRR) (nondestructive method). We found clear evidence that three characteristic temperature ranges govern how the mechanism of the SiO_2/Si interface roughening switches above the viscous-flow temperature of SiO_2.

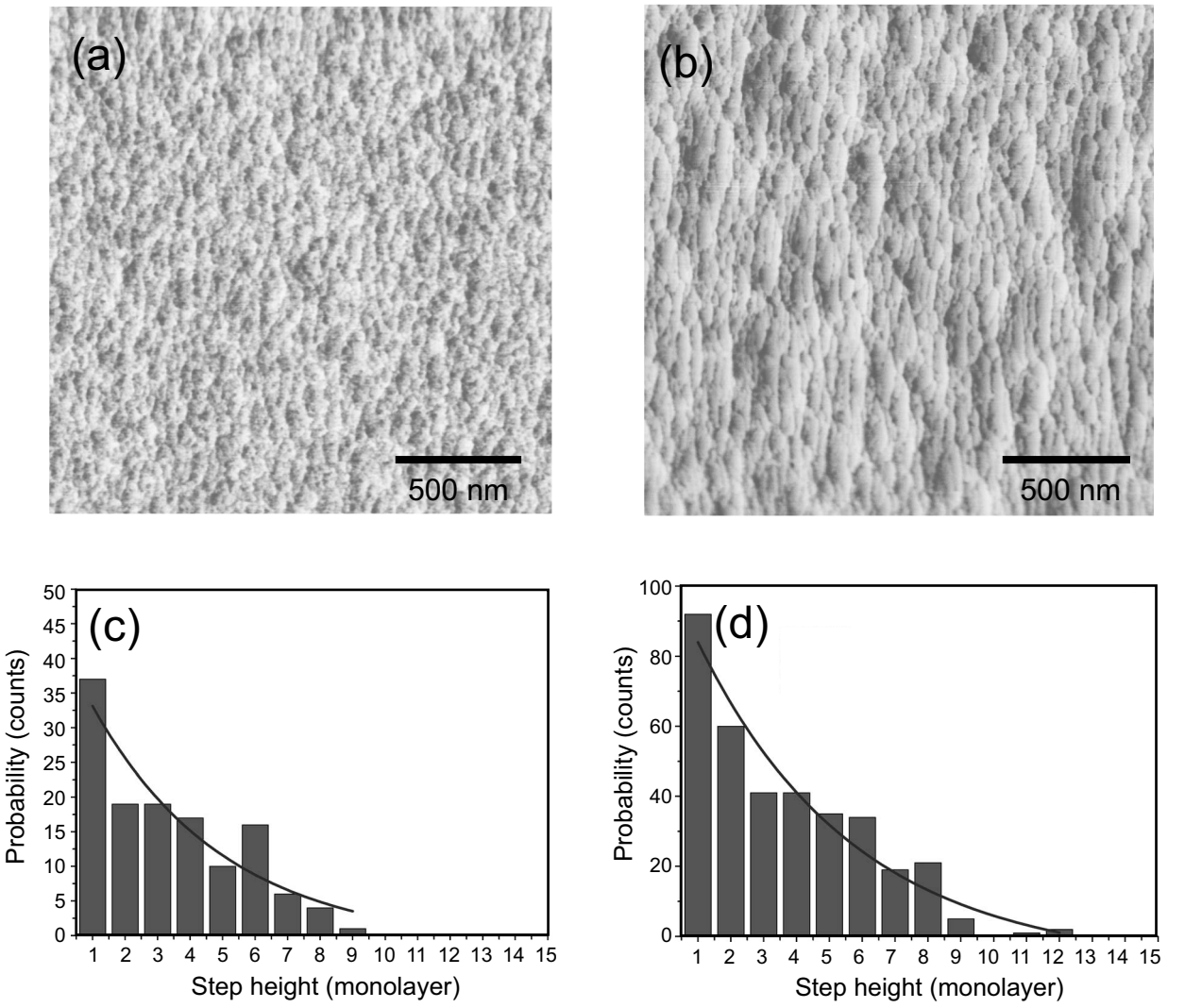

FIG. 1. AFM images of the Si(001) surface after thermal oxidation at (a) 1200 °C and (b) 1325 °C, followed by chemical etching. The image size is 2×2 μm^2. The full topographic scale, 5.0 nm, is shown. (c) and (d) are distributions of step height at the interfaces in (a) and (b), respectively. Solid lines are exponential fitting curves.

II. EXPERIMENTAL

We used B-doped Si(100) wafers (resistivity $=1-10$ Ω cm) with miscut angle θ of 0.1°, 0.5°, 1.0°, 2.0°, 3.0°, or 4.0° toward the [110] direction. The wafers were thermally oxidized in a conventional electronic furnace. Before introducing the wafers into the furnace, we etched them in 1% HF and 99% doubly deionized (DDI) H_2O by volume to remove native silicon oxide layers. The wafers were subjected to various annealing conditions in an Ar atmosphere containing a small constant fraction of O_2 gas (0.20 ± 0.01 %). Throughout the experiments, the Ar flow rate was kept constant at 2.0 l/min. The rate of heating and cooling from the base furnace temperature of 600 °C was 5 °C/min or less. The annealing temperature and the time were 1000–1380 °C and <50 h, respectively. The annealing conditions we used are in the passive oxidation regime, not in the active oxidation regime.[5,14] Following the annealing treatment, the samples were etched in 0.5% HF and 99.5% DDI H_2O by volume for 2–20 min to remove the silicon oxide layers. Morphologies at the interface were observed in air by tapping-mode AFM immediately after the removal of the as-grown silicon oxide layers.

XRR measurements of the samples thermally oxidized in the furnace were performed by using the z-axis goniometer at beamline BL24XU of SPring-8.[20] The 0.124 nm x-ray wavelength was used at the incident angle by varying the angle from 0.1° to 4.0°. Before the x-ray beam entered the goniometer, it had been monochromatized and collimated to 0.1 (V) and 1.0 mm (H) dimensions by using x-y slits; the scattered beam was confined by a 0.3 mm slit. A NaI detector was used to detect reflectivity from the samples.

III. RESULTS AND DISCUSSION

Figure 1 shows AFM images of the interfaces between thermal silicon oxide layers grown at the oxidation temperatures (T_{ox}) of 1250 °C and 1325 °C in a 0.2% O_2-Ar mixture and the Si(001) substrate with a miscut angle of 1.0°

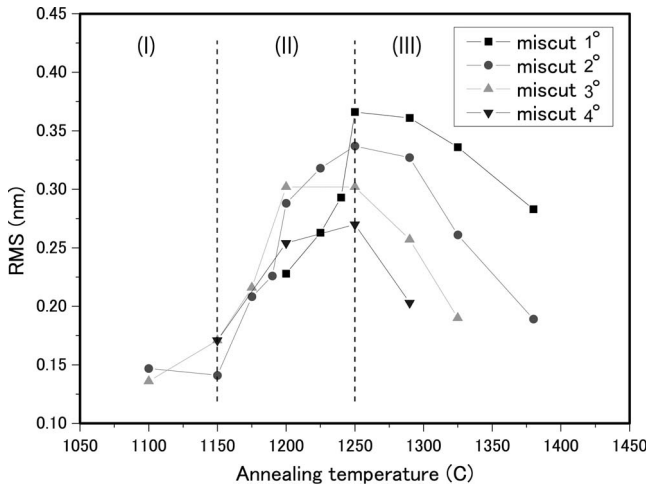

FIG. 2. rms vs oxidation temperature. Samples miscut at several angles were thermally oxidized in the 0.2% oxygen-Ar mixture for 2.5 h. Three characteristic regions are labeled (I), (II), and (III) with respect to the oxidation temperature.

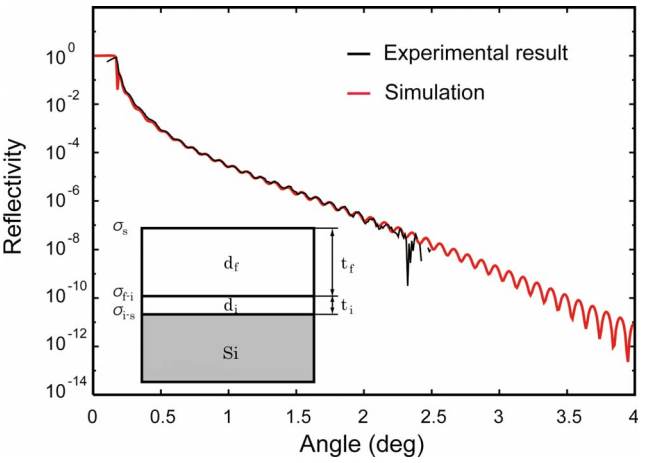

FIG. 3. (Color online) Black line: a representative XRR profile of the sample thermally oxidized in the 0.2% oxygen mixture at $T_{ox}=1250$ °C for 4 h. Note that the background intensities are subtracted in the profile. Red line: best-fit profile obtained with the two-layer model which is schematically shown in the inset. The simulation fits the experimental data well assuming that the density of silicon oxide bulk film is equal to the silica glass density of 2.206 g/cm^3 (Ref. 22). The fitting error R is 0.0349. The fitting error is defined as $R=\Sigma_l|\ln I^{obs}(l)-\ln I^{cal}(l)|/\Sigma_l|\ln I^{obs}(l)|$ where $I^{obs}(l)$ and $I^{cal}(l)$ are, respectively, the reflectivities in experiments and calculations at the angle of l.

($t=2.5$ h). As can be seen in these images, the interface is composed of step-and-terrace structures at 1250 °C [Fig. 1(a)] and 1325 °C [Fig. 1(b)], but it is rough without step-and-terrace structures at 1100 °C [not shown here]. This indicates that a morphological transition occurs between 1100 °C and 1250 °C, which is related to the diffusion length of silicon species at the interface as we reported in Ref. 5. We can also see that there is a clear morphological difference between 1250 °C and 1325 °C [compare Figs. 1(a) and 1(b)]. The edges of the interface steps at $T_{ox}=1250$ °C are not straight but wiggly, while those at $T_{ox}=1325$ °C are straighter than those at $T_{ox}=1250$ °C. Figures 1(c) and 1(d) show the step height distributions at the interfaces at $T_{ox}=1250$ °C and 1300 °C, respectively. The step heights are exponentially distributed from one monolayer to several ten monolayers in height at $T_{ox}=1250$ °C and $T_{ox}=1325$ °C, but the probability of one monolayer height at $T_{ox}=1325$ °C is higher than that at $T_{ox}=1250$ °C. This indicates that the high-temperature oxidation above 1250 °C not only causes the formation of the multiple interfacial steps but also simultaneously smoothens the interface features at $t=2.5$ h.

Figure 2 shows the temperature dependence of roughness at the interface between thermal SiO_2 grown in 0.2% O_2-Ar mixture for 2.5 h and the silicon substrates with miscut angles below 4° obtained by AFM. The interface, as seen in Fig. 2, becomes rough due to the formation of interfacial multiple step structures [Fig. 1] at $T_{ox}>1150$ °C and has the maximum roughness at $T_{ox}=1250$ °C. The temperature-dependent roughening can therefore be categorized into three regions with respect to growth temperature: (I) $T_{ox}<1150$ °C, where roughness is constant; (II) 1150 °C$<T_{ox}<$1250 °C, where roughness sharply increases as oxidation temperature increases and is maximum at 1250 °C independent of miscut angles below 4°; and (III) 1250 °C$<T_{ox}<$1380 °C, where the interface roughness gradually decreases, that is, the roughened interface becomes smooth during the oxidation as the oxidation temperature increases, in accordance with the AFM results in Fig. 1. There is maximum roughness at around 1250 °C, meaning that there are competing mechanisms causing the roughening and smoothening as discussed below.

To understand the mechanism of the temperature dependence underlying the interface roughening and smoothening, we performed XRR measurements using synchrotron-radiation light on the samples with $\theta=0.1°$ grown at high temperatures between 1000 °C and 1380 °C. In the calculation of the XRR profiles,[21] we used the following parameters: silicon oxide bulk film density ($d_f=2.206$ g/cm^3),[22] dense interfacial transition layers density (d_i), silicon substrate density ($d_{Si}=2.316$ g/cm^3), roughness at the surface (σ_f) and interfaces between silicon oxide bulk film and interfacial transition layers ($\sigma_{f\text{-}i}$) and between interfacial transition layers and silicon substrate ($\sigma_{i\text{-}s}$), and the thickness of silicon oxide bulk film (t_f) and that of the interfacial transition layers (t_i) in the two-layer model.[23] A representative profile at $T_{ox}=1250$ °C is shown in Fig. 3. The experimental XRR profile and the simulation fit well with the fitting error $R=0.0349$. This indicates that the there exist dense ($d_i=2.35$ g/cm^3) and thin ($t_i=1.1$ nm) interfacial transition layers at the interface between silicon oxide bulk film ($t_f=34.72$ nm) and silicon substrate as in the case of low-temperature oxidation. We plot the fitting parameters of the samples oxidized at different temperatures in Figs. 4(a)–4(c).

As seen in Fig. 4(a), $\sigma_{i\text{-}s}$ is constant in region (I), but it becomes extremely rough from $T_{ox}=1150$ °C with the roughness reaching a maximum at $T_{ox}=1250$ °C in region (II). It then gradually becomes smaller in region (III), in accordance with the AFM results in Fig. 2. This supports the validity of the fitting analyses using the assumption of

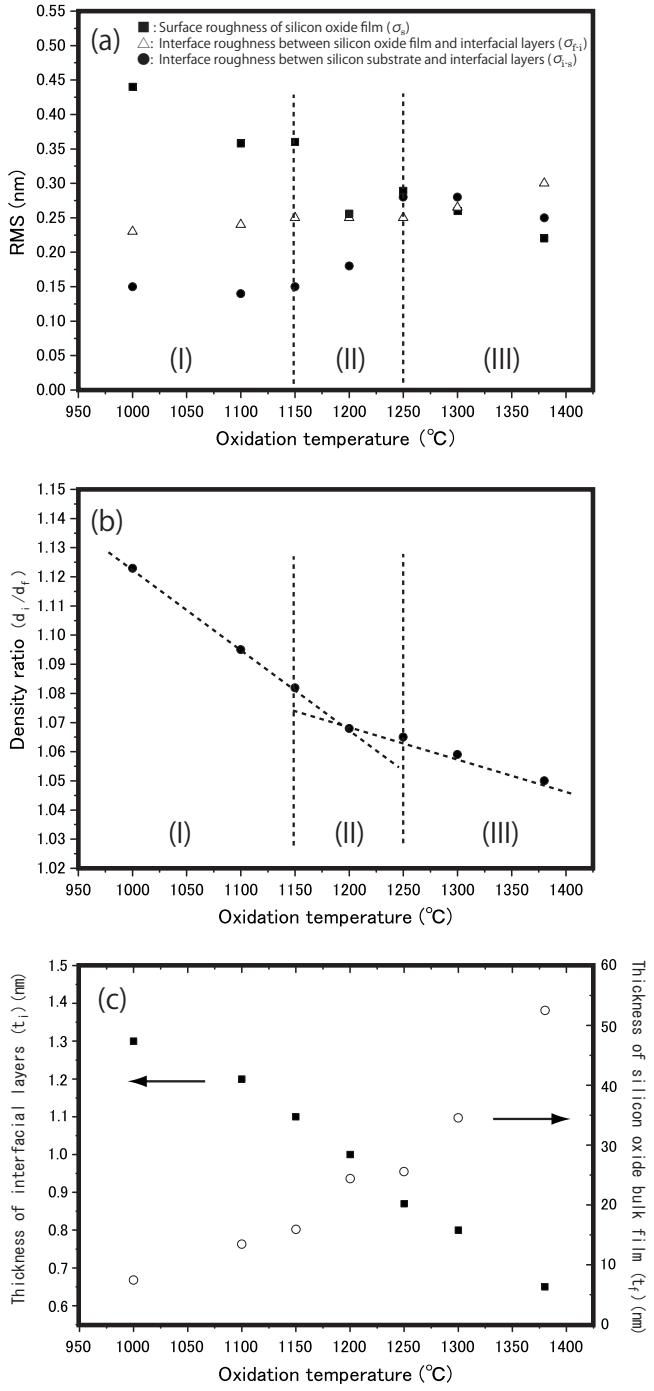

FIG. 4. Plots of best-fit parameters for XRR measurements on samples grown at oxidation temperatures between 1000 °C and 1380 °C in the 0.2% O_2/Ar mixture. (a) Roughness at the surface and the interfaces of the film as a function of oxidation temperature. (b) Density ratio between interfacial transition layers and silicon oxide film. Dotted lines are two types of linear fittings. (c) Thickness of interfacial transition layers and silicon oxide bulk films.

d_f=2.206 g/cm^3. In contrast to $\sigma_{i\text{-}s}$, the surface roughness of the silicon oxide bulk film (σ_f), which has the largest roughness in the interfaces of the films at $T_{ox}<1250$ °C, becomes smaller in regions (I) and (II) with some modulations and behaves as $\sigma_{i\text{-}s}$ in region (III) (it finally becomes nearly equal to $\sigma_{i\text{-}s}$ at 1380 °C). $\sigma_{f\text{-}i}$, on the other hand, is almost constant in regions (I) and (II), but the interface becomes slightly rough above 1250 °C (e.g., $\sigma_{f\text{-}i}^{1380}/\sigma_{f\text{-}i}^{1100}=1.21$), and the roughness finally becomes the largest at 1380 °C ($\sigma_{f\text{-}i}^{1380}=0.3$ nm, which is nearly equal to $\sigma_{i\text{-}s}^{1250}$).

The density ratio between the interfacial transition layers and the silicon oxide bulk film (d_i/d_f), which is larger than unity, reduces from 1.12 to 1.05 between 1000 °C and 1380 °C [Fig. 4(b)], while t_i gradually reduces as T_{ox} increases ($t_i^{1000}=1.3$ nm and $t_i^{1380}=0.85$ nm) [Fig. 4(c)].[24] This indicates that the planar density of the transition layers d_s, which is defined as $d_i t_i$, becomes smaller with T_{ox}. Interestingly, as seen in Fig. 4(b), the ratio can be fitted linearly in two ways: one is between 1000 °C and 1200 °C and the other is between 1200 °C and 1380 °C. There is a clear slope change in the linear fittings at $T_{ox}=1200$ °C, suggesting that there is a transition in density inside the silicon oxide bulk films and that there are two different mechanisms that reduce d_i in region (II). The transition temperature indeed nearly corresponds to the onset of the glass transition of fused silica (~1200 °C) or quartz (~1175 °C).[25]

On the basis of the AFM and the XRR results, the remarkable temperature dependence of oxidation kinetics at the SiO_2/Si(001) interface can be explained as follows: the reduction in the density and the thickness of the interfacial transition layers with increasing T_{ox} indicates that the stress generated by the high-temperature oxidation (>1100 °C) is mainly relieved in the interfacial transition layers. The oxidation-induced stress at the interface therefore becomes smaller as T_{ox} increases. In region (I) (below 1100 °C), where lateral diffusion of silicon species at the interface is negligibly small,[18] the oxidation-induced stress between the silicon oxide bulk films and the interfacial transition layers is balanced via the relaxation of stress in the transition layers, because $\sigma_{f\text{-}i}$ is almost constant in this region [Fig. 4(a)]. The high degree of σ_f is indicative of the small degree of viscosity of the oxide film compared to that of the interfacial transition layers, although it becomes smaller with increasing T_{ox}. In region (II), the lateral diffusion of silicon species becomes prominent at the $SiO_x(i)$-Si interface.[18] As a result, the strain induced by the oxidation is relieved through the dense and high-viscosity interfacial transition layers not only perpendicular to but also parallel to the $SiO_x(i)$-Si interface. If the strains in the transition layers have local distribution parallel to the interface, the strain distribution can modulate the diffusion of oxygen and thus change the local reaction rate at the interface, which can lead to the formation of multiple steps at the interface via layer-by-layer growth,[3] resulting in the increase in $\sigma_{i\text{-}s}$. In region (III), the relaxation of the oxidation-induced stress in the silicon oxide bulk film possibly plays an important role in the decrease in $\sigma_{i\text{-}s}$. σ_f and $\sigma_{i\text{-}s}$ become almost the same (0.3 nm) at $T_{ox}=1250$ °C and then coincidently become smaller with increasing T_{ox}, while $\sigma_{f\text{-}i}$ gradually increases in region (III) [Figs. 4(a)–4(c)]. The results indicate that the oxide film and the interface transition layers act together at $T_{ox}>1250$ °C and imply that the oxidation-induced strain is homogeneously relaxed not only in the interfacial transition layers but also in the whole region of the silicon oxide bulk films by relaxation via viscosity flow in the silicon oxide bulk film with high-temperature

annealing. This feature is consistent with the presence of the transition in the density of the interfacial transition layers at 1200 °C [Fig. 4(b)]. The homogeneous strain distribution in the silicon oxide bulk film via viscous flow causes the uniform reaction rate at the interface. This explains the onset of the smoothening of the $SiO_x(i)$-Si interface and the smoothening of the surface of silicon oxide bulk films as described in the next paragraph.

Finally, we discuss the stress effect on the oxidation kinetics that governs the interface roughening and smoothening. According to Ref. 18, Eq. (2) suggests that there is competition between the linear terms $\nabla^2 h$ and $\nabla^4 h$ generating the characteristic horizontal length $L_1=(D/\mu)^{1/2}$.[1] The characteristic length actually appears in the phase transition from disordered to step-terrace structures at $T_{ox}=1200$ °C. However, the onset of smoothening above 1250 °C in region (III) is not explained by this equation, suggesting that we are missing an additional term in Eq. (2). According to Ref. 26, on the other hand, the equation of oxidation kinetics below the viscous-flow temperature should include the $G|\nabla h|$ term in a planar-interface approximation,[27] which describes the stress effect on the instability of the planar interface [as in Eq. (13) in Ref. 26(a)], where G is a constant. It is therefore reasonable to assume that there is an effect on the interface stability, since we actually observed the high-density interfacial transition layers even at high-temperature oxidation [Fig. 4(c)]. By adding the $G|\nabla h|$ term as in Eq. (3) below, we can understand the temperature dependence as follows: in region (I), judging from the fact that the roughness is small independent of T_{ox}, the $\nabla^2 h$ term is dominant as was observed in Refs. 4 and 5, meaning that the stress exists at the interface but the term is not activated,

$$\frac{\partial h(\mathbf{r},t)}{\partial t} = \mu\nabla^2 h(\mathbf{r},t) - D\nabla^4 h(\mathbf{r},t) + G|\nabla h| + \eta(\mathbf{r},t). \quad (3)$$

In region (II), $\nabla^4 h$ becomes dominant at $T_{ox}=1200$ °C, which causes the formation of the step-terrace structure.[18] The further increase in $\sigma_{i\text{-}s}$ between $T_{ox}=1200$ °C and 1250 °C [Fig. 4(a)] is possibly due to the emergence of the strain effect that enhances the contribution of the $|\nabla h|$ term. In region (III), however, the contribution from $\nabla^4 h$ switches to the $|\nabla h|$ term in the roughening. The analyses by Grinstein *et al.* showed that the constant G multiplied to the $|\nabla h|$ term is proportional to the interface stress as in Eq. (13) in Ref. 26(a). Since we observed that the strain is relieved in the silicon oxide bulk films [Fig. 4(a)], the relaxation of strain reduces this constant and thus the contribution from the strain term becomes smaller with increasing T_{ox}, while the contribution from the smoothening term, the $\nabla^2 h$ term and/or $\nabla^4 h$, becomes dominant again. The emergence and reduction in the strain effect reasonably explains the transition from roughening to smoothening at the $SiO_x(i)$-Si interface at $T_{ox}=1250$ °C.

IV. CONCLUSION

In conclusion, we discovered a temperature-dependent morphological instability-stability transition at the SiO_2/Si(001) interface during thermal silicon oxidation above 1100 °C in dilute oxygen atmosphere in a furnace. The transition implies a strain effect on the oxidation kinetics at the interface between the dense and the thin interfacial transition layers and the substrate at oxidation temperatures above 1250 °C.

*Corresponding author; homi@will.brl.ntt.co.jp
†Present address: Nichia Corporation.
‡Present address: Keio University.
§Present address: Osaka University.
‖Present address: JAEA.

[1] A.-L. Barabási and H. E. Stanley, *Surface Growth* (Cambridge University Press, Cambridge, England, 1995).
[2] J. Dabrowski and H.-J. Müssig, *Silicon Surfaces and Formation of Interfaces* (World Scientific, Singapore, 2000), Chap. 6.
[3] *Fundamental Aspects of Silicon Oxidation*, edited by Y. J. Chabal (Springer, New York, 2001).
[4] H. Cui, C. X. Wang, and G. W. Yang, Nano Lett. **8**, 2731 (2008).
[5] M. A. Albao, D. J. Liu, C. H. Choi, M. S. Gordon, and J. W. Evans, Surf. Sci. **555**, 51 (2004).
[6] B. E. Deal and A. S. Grove, J. Appl. Phys. **36**, 3770 (1965).
[7] H. Kageshima and K. Shiraishi, Phys. Rev. Lett. **81**, 5936 (1998).
[8] M. Uematsu, H. Kageshima, Y. Takahashi, S. Fukatsu, K. M. Itoh, and K. Shiraishi, Appl. Phys. Lett. **84**, 876 (2004).
[9] T. Watanabe, K. Tatsumura, and I. Ohdomari, Phys. Rev. Lett. **96**, 196102 (2006).
[10] T. Watanabe and I. Ohdomari, J. Electrochem. Soc. **154**, G270 (2007).
[11] H. Cui, Y. Sun, G. Z. Yang, and C. X. Wang, Appl. Phys. Lett. **94**, 083108 (2009).
[12] For example, Y. Enta, B. S. Mun, M. Rossi, P. N. Ross, Jr., Z. Hussian, C. S. Fadley, K.-S. Lee, and S.-K. Kim, Appl. Phys. Lett. **92**, 012110 (2008).
[13] For example, A. Bongiorno and A. Pasquarello, Phys. Rev. B **70**, 195312 (2004).
[14] Y. Takakuwa, M. Nihei, and N. Miyamoto, Appl. Surf. Sci. **117-118**, 141 (1997).
[15] L. Lai and E. A. Irene, J. Appl. Phys. **86**, 1729 (1999).
[16] X. Chen and J. M. Gibson, Phys. Rev. Lett. **81**, 4919 (1998); J. Vac. Sci. Technol. A **17**, 1269 (1999); J. Electrochem. Soc. **146**, 3032 (1999).
[17] D. J. Bottomley, H. Omi, Y. Kobayashi, M. Uematsu, H. Kageshima, and T. Ogino, Phys. Rev. B **66**, 035301 (2002).
[18] H. Omi, H. Kageshima, and M. Uematsu, Phys. Rev. Lett. **97**, 016102 (2006).
[19] A. R. Chowdhuri, D.-U. Jin, J. Rosado, and C. G. Takoudis, Phys. Rev. B **67**, 245305 (2003).
[20] H. Omi, T. Kawamura, S. Fujikawa, Y. Tsusaka, Y. Kagoshima, and J. Matsui, Appl. Phys. Lett. **86**, 263112 (2005).
[21] *X-ray and Neutron Reflectivity: Principles and Applications*, edited by J. Daillant and A. Gibaud (Springer, Heidelberg, 1999).

[22] M. Castro-Colin, W. Donner, S. C. Moss, Z. Islam, S. K. Sinha, and R. Nemanich, Phys. Rev. B **71**, 045311 (2005).

[23] N. Awaji, S. Ohkubo, T. Nakanishi, Y. Sugita, K. Takasaki, and S. Komiya, Jpn. J. Appl. Phys., Part 2 **35**, L67 (1996).

[24] Note here that we have confirmed that d_i/d_f is constant with respect to the total silicon oxide film thickness (t_i+t_f) at a T_{ox} within our experimental condition $(8.8<t_i+t_f<54$ nm), which will be present elsewhere.

[25] P. P. Donnadieu, O. Jaoul, and M. Kleman, Philos. Mag. A **52**, 5 (1985).

[26] (a) G. Grinstein, Yuhai Tu, and J. Tersoff, Phys. Rev. Lett. **81**, 2490 (1998); (b) **83**, 657 (1999); (c) V. P. Zhdanov, *ibid.* **83**, 656 (1999).

[27] According to Ref. 26, a simple algebraic calculation shows that the strain term in Eq. (11) in Ref. 26, which is proportional to $w_1 q \alpha_q \cos(qx)$, is equal to $w_1 \left| \frac{(\partial h/\partial x)^2+\sqrt{(\partial h/\partial x)^4+4\alpha_q^2(\partial^2 h/\partial x^2)^2}}{2} \right|^{1/2}$, where the interface position is $h(x,t)=h_0(x,t)+\alpha_q(t)\cos(qx)$, with $h_0(x,t)$ being its average position, $\alpha_q(t)$ as the amplitude of the interface at time t, and $2\pi/q$ as the wavelength. Thus, the strain term nearly equals to $w_1|\partial h/\partial x|$ in the case of planar-interface approximation $(\alpha_q \approx 0)$.